Electromagnetic Scattering From Vegetation Cylindrical Components

V. Santalla del Rio, *Member, IEEE*, L. Abalde-Lima, and C. G. Christodoulou, *Fellow, IEEE*

***Abstract*—An approach for calculating electromagnetic scattering, valid in the near- and far-field regions, from a homogeneous finite cylindrical vegetation sample at oblique incidence is presented and discussed. The proposed solution will help in taking into account multiple scattering effects due to plant structure. It does not require assumptions on the dimensions or electromagnetic properties of the vegetation cylinder.**

***Index Terms*—Forest remote sensing, scattering matrix.**

I. Introduction

ACCURATE estimation of electromagnetic scattering from vegetation is of interest for remote sensing applications as well as for communications to improve attenuation calculations. Since many of the elemental scatterers found in vegetation media can be approximated by cylinders, computation of electromagnetic scattering from cylinders at oblique incidence is important.

In 1955, Wait [1] presented a general solution for the electromagnetic scattering from a homogeneous infinite circular cylinder, at oblique incidence. No assumptions about the complex dielectric constant are made. The given solution is valid for the entire space. Recently, this solution has been used in [2] to obtain the far-field scattering matrix of a finite dielectric cylinder at oblique incidence. Being based on the solution for an infinite cylinder, the solution proposed is valid for cylinders with large length-to-radius ratios. This far-field solution has been widely reviewed and validated in [3] and [4]. Also, it has been routinely used when developing vegetation scattering models [5]–[7]. However, it cannot be used if vegetation elements are in the near field of each other, and second-order scattering contributions cannot be neglected [8], [9]. At low frequencies and/or for some dense vegetation fields, as most cultivated crop fields are, multiple scattering and near-field effects cannot be neglected. The solution provided in [10] allows calculation of scattering in the near field with respect to the cylinder length dimension but requires the cylinder length to be long with respect to the wavelength and, to be in the far-field region, with respect to the cylinder diameter. In this letter, a new approach for finite cylinder scattering calculations is explored. It is valid in both whole near- and far-field regions, making in it a good solution for high and low frequencies when the vegetation elements are close to each other and second-order scattering must be taken into account. The approach to be presented considers an infinite cylinder illuminated by a plane wave. The incident field on the cylinder is "windowed," so that it is zero outside the actual finite length cylinder. Spectral decomposition of this field on the cylinder surface and application of boundary conditions allow obtaining the scattered field. The next section describes the problem and discusses the approach to implementation, pointing out its limitations and advantages. Then, in Section III, the mathematical development of the approach is introduced. Finally, results and conclusions are presented and discussed.

Manuscript received May 12, 2014; revised August 20, 2014 and September 12, 2014; accepted September 27, 2014. This work was supported in part by the European Regional Development Fund and the Galician Regional Government under Project CN 2012/260 "Consolidation of Research Units: Atlantic" and in part by the Spanish State Secretary for Research under Project TEC2011-28789-C02-02.

V. Santalla del Rio and L. Abalde-Lima are with Teoría de la Señal y Comunicaciones, Universidad de Vigo, 36310 Vigo, Spain.

C. G. Christodoulou is with the Department of Electrical and Computer Engineering, The University of New Mexico, Albuquerque, NM 87131 USA.

Digital Object Identifier 10.1109/LGRS.2014.2361066

II. Problem and Approach Description

The homogeneous finite length cylinder in the Cartesian reference system ($\hat{x}$, $\hat{y}$, $\hat{z}$) is shown in Fig. 1. The cylinder, with length L, radius a, and relative complex dielectric constant ϵ_r, is placed in free space.

Assuming an angular frequency $w = 2\pi f$ and a time harmonic dependence of the form $e^{-j\omega t}$ (which has been suppressed for simplicity), the incident homogeneous plane wave can be expressed as

$$\vec{E}_i = E_0 \cdot e^{jk_o \hat{k}_i \vec{r}} \hat{p}_i \tag{1}$$

where $k_o = w\sqrt{\mu_o \epsilon_o}$ is the free space wavenumber with μ_o and ϵ_o as the free space permeability and permittivity, respectively, $\hat{k}_i = \sin\theta_i \cos\phi_i \hat{x} + \sin\theta_i \sin\phi_i \hat{y} + \cos\theta_i \hat{z}$ is the unit vector in the incident direction, and $\hat{p}_i$ is the incident field polarization unit vector. It can be either horizontal $\hat{h}_i$ or vertical $\hat{v}_i$

$$\begin{aligned} \hat{h}_i &= \frac{\hat{z} \times \hat{k}_i}{|\hat{z} \times \hat{k}_i|} = -\sin\phi_i \hat{x} + \cos\phi_i \hat{y} \\ \hat{v}_i &= \hat{h}_i \times \hat{k}_i = \cos\theta_i \cos\phi_i \hat{x} + \cos\theta_i \sin\phi_i \hat{y} - \sin\theta_i \hat{z}. \end{aligned} \tag{2}$$

For the scattered field, the unit vector in the scattering direction $\hat{k}_s$ and its corresponding horizontal and vertical polarization unit vectors $\hat{h}_s$ and $\hat{v}_s$ will be given by

$$\begin{aligned} \hat{k}_s &= \sin\theta_s \cos\phi_s \hat{x} + \sin\theta_s \sin\phi_s \hat{y} + \cos\theta_s \hat{z} \\ \hat{h}_s &= \frac{\hat{z} \times \hat{k}_s}{|\hat{z} \times \hat{k}_s|} = -\sin\phi_s \hat{x} + \cos\phi_s \hat{y} \\ \hat{v}_s &= \hat{h}_s \times \hat{k}_s = \cos\theta_s \cos\phi_s \hat{x} + \cos\theta_s \sin\phi_s \hat{y} - \sin\theta_s \hat{z}. \end{aligned} \tag{3}$$

Let us consider an infinite cylinder that contains the cylinder of interest shown in Fig. 1. The scattered field from this infinite cylinder can be calculated, as shown in [1] and [2] by applying the boundary conditions on the cylinder surface and assuming that both internal and scattered fields can be expressed as a sum of cylindrical waves. By denoting the internal field inside the

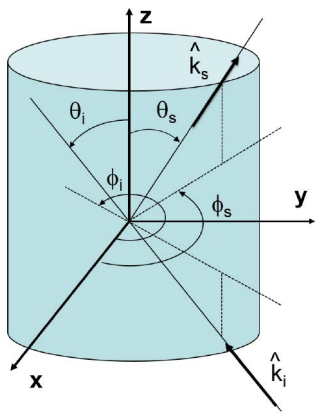

Fig. 1. Cylinder reference system.

infinite cylinder as $\vec{E}_{\rm int}$ and the scattered field outside it as $\vec{E}_s$, the boundary conditions lead to

$$\hat{\rho}\times\left(\vec{E}_{\rm int}-\vec{E}_s\right)|_{\rho=a}=\hat{\rho}\times\vec{E}_i|_{\rho=a} \quad (4)$$

$$\hat{\rho}\times\left(\vec{H}_{\rm int}-\vec{H}_s\right)|_{\rho=a}=\hat{\rho}\times\vec{H}_i|_{\rho=a} \quad (5)$$

where $\vec{E}_{\rm int}$ is expressed in terms of incoming cylindrical waves $R_g\overline{M_n}(k_z,k_{c\rho})$ and $R_g\overline{N_{\rm n}}(k_z,k_{c\rho})$ [3]

$$\vec{E}_{\rm int}=\int\sum_{n=-\infty}^{\infty}\left(C_n^m(k_z)R_g\overline{M_n}(k_z,k_{c\rho})+C_n^n(k_z)R_g\overline{N_n}(k_z,k_{c\rho})\right)dk_z \quad (6)$$

and, correspondingly, the scattered field is expressed in terms of outgoing cylindrical waves $\overline{M_n}(k_z,k_\rho)$ and $\overline{N_n}(k_z,k_\rho)$

$$\vec{E}_s=\int\sum_{n=-\infty}^{\infty}\left(S_n^m(k_z)\overline{M_n}(k_z,k_\rho)+S_n^n(k_z)\overline{N_n}(k_z,k_\rho)\right)dk_z \quad (7)$$

where $k_{c\rho}=\sqrt{k_c^2-k_z^2}$, $k_c=w\sqrt{\mu_o\epsilon_o\epsilon_r}$, and $k_\rho=\sqrt{k^2-k_z^2}$.

The coefficients of the scattered cylindrical waves $S_n^m(k_z)$ and $S_n^n(k_z)$ and those of the internal cylindrical waves $C_n^m(k_z)$ and $C_n^n(k_z)$ can be obtained from the boundary conditions if the tangential components of the surface fields on the cylinder due to the incident wave are known. For an incident plane wave, which is vertically polarized, these are

$$\begin{aligned}\vec{E}_i^{v\parallel}(\rho=a)&=e^{jk_{iz}z}e^{jk_{i\rho}a\cos(\phi_i-\phi)}\cdot\left(\cos\theta_i\sin(\phi_i-\phi)\hat{\phi}-\sin(\theta_i)\hat{z}\right)\\ \vec{H}_i^{v\parallel}(\rho=a)&=\frac{k}{w\mu}e^{jk_{iz}z}e^{jk_{i\rho}a\cos(\phi_i-\phi)}\cos(\phi_i-\phi)\hat{\phi}\end{aligned} \quad (8)$$

with $k_{iz}=k_o\cos\theta_i$ and $k_{i\rho}=k_o\sin\theta_i$. Moreover, for a horizontally polarized wave, the surface fields become

$$\begin{aligned}\vec{E}_i^{h\parallel}(\rho=a)&=e^{jk_{iz}z}e^{jk_{i\rho}a\cos(\phi_i-\phi)}\cos(\phi_i-\phi)\hat{\phi}\\ \vec{H}_i^{h\parallel}(\rho=a)&=\frac{-k}{w\mu}e^{jk_{iz}z}e^{jk_{i\rho}a\cos(\phi_i-\phi)}\cdot\left(\cos\theta_i\sin(\phi_i-\phi)\hat{\phi}-\sin(\theta_i)\hat{z}\right).\end{aligned} \quad (9)$$

Now, $S_n^m(k_z)$, $S_n^n(k_z)$, $C_n^m(k_z)$, and $C_n^n(k_z)$ can be easily calculated from the linear equation systems that result if field expressions (6), (7), and (8) or (9) are substituted in the equations given by the boundary conditions on the cylinder surface. Thus, both internal and scattered fields from an infinite cylinder are obtained as shown in [1]. Based on this solution, an approximation for obtaining the scattered field from a finite length cylinder was proposed in [2]. This solution, which is valid in the far-field region, is based on integrating the internal field of the infinite cylinder inside the finite cylinder using the Helmholtz integral equation. Since the internal fields of the finite cylinder are approximated by the internal fields of the infinite cylinder, this approximation is valid for finite cylinders with large length-to-radius ratio. The same approach was considered in [3], although here, the Helmholtz integral is performed only over the cylindrical surface of the finite cylinder, consequently neglecting radiation from the top ends.

The approximation to be proposed is different from those proposed in [2] and [3]. In those cases, it was proposed "to window" the internal field in the infinite cylinder to calculate the scattered field from the finite cylinder, i.e., the internal fields of the infinite cylinder that are outside the actual finite cylinder of interest are neglected. In here, it is proposed "to window" the incident field on the infinite cylinder surface before calculating the scattered and internal fields of the infinite cylinder. That is, any incident field on the infinite cylinder surface, outside the cylindrical surface of the actual finite cylinder, will be neglected. Evidently, this approach implies neglecting the scattering/radiation from the cylinder top ends and the diffracted fields from the cylindrical surface limits of the finite cylinder. Neglecting these contributions may be unacceptable for some applications. However, if we consider the structure of most vegetation media, where the elemental scatterers are connected through their ends or to the ground and, thus, scattering from these ends is not important as they are usually blocked by the ground, other branches, or other smaller vegetation elements as leaves, it looks reasonable to neglect those contributions. In return, the scattered field solution will be valid in the near- and far-field regions.

III. Approximation to the Scattered Field From a Cylinder

Considering the proposed approach, the boundary conditions to be met on the cylinder surface can be expressed as

$$\hat{\rho}\times\left(\vec{E}_{\rm int}-\vec{E}_s\right)=\begin{cases}\hat{\rho}\times\vec{E}_i, & |z|<=L/2,\rho=a\\ 0, & |z|>L/2,\rho=a\end{cases} \quad (10)$$

$$\hat{\rho}\times\left(\vec{H}_{\rm int}-\vec{H}_s\right)=\begin{cases}\hat{\rho}\times\vec{H}_i, & |z|<=L/2,\rho=a\\ 0, & |z|>L/2,\rho=a.\end{cases} \quad (11)$$

Since both internal and scattered fields of the cylinder surface are expressed in terms of cylindrical functions, i.e., in terms of exponential functions of z and ϕ, to obtain the scattered field from solving for the boundary conditions (10) and (11), the fields on the cylinder surface need to be expanded in terms of exponential functions on z and ϕ. This can be achieved by means of the transformation pair

$$\begin{aligned}\vec{V}(z,\phi)&=\int_{-\infty}^{\infty}\sum_{n=-\infty}^{\infty}\vec{F}_n(k_z)e^{jk_zz}e^{jn\phi}dk_z\\ \vec{F}_n(k_z)&=\frac{1}{4\pi^2}\int_{-\infty}^{\infty}\int_{-\pi}^{\pi}\vec{V}(z,\phi)e^{-jk_zz}e^{-jn\phi}d\phi\,dz.\end{aligned} \quad (12)$$

Doing so, for the proposed approach, the tangential components of the incident electric and magnetic fields on the cylinder surface can be expressed as

$$\vec{E}_i^{v\|}(\rho=a)=\int_{-\infty}^{\infty}\sum_{n=-\infty}^{\infty}\vec{F}_n^v(k_z)e^{jk_zz}e^{jn\phi}dk_z \tag{13}$$

$$\vec{E}_i^{h\|}(\rho=a)=\int_{-\infty}^{\infty}\sum_{n=-\infty}^{\infty}\vec{F}_n^h(k_z)e^{jk_zz}e^{jn\phi}dk_z \tag{14}$$

$$\vec{H}_i^{v\|}(\rho=a)=\int_{-\infty}^{\infty}\sum_{n=-\infty}^{\infty}\frac{k}{w\mu}\vec{F}_n^h(k_z)e^{jk_zz}e^{jn\phi}dk_z \tag{15}$$

$$\vec{H}_i^{h\|}(\rho=a)=\int_{-\infty}^{\infty}\sum_{n=-\infty}^{\infty}\frac{-k}{w\mu}\vec{F}_n^v(k_z)e^{jk_zz}e^{jn\phi}dk_z \tag{16}$$

where $\vec{F}_n^v(k_z)$ and $\vec{F}_n^h(k_z)$ have been found to be

$$\vec{F}_n^v(k_z)=\frac{j^n}{2\pi}e^{-jn\phi_i}J_n(k_{i\rho})L\,\mathrm{sinc}\left(\frac{(k_z-k_{iz})L}{2\pi}\right)\cdot\left(\cos\theta_i\frac{n}{k_{i\rho}a}\hat{\phi}-\sin\theta_i\hat{z}\right) \tag{17}$$

$$\vec{F}_n^h(k_z)=\frac{j^{(n-1)}}{2\pi}e^{-jn\phi_i}J_n'(k_{i\rho}a)L\,\mathrm{sinc}\left(\frac{(k_z-k_{iz})L}{2\pi}\right)\hat{\phi}. \tag{18}$$

Then, in the case of a vertically polarized incident wave, the application of the boundary conditions will lead to

$$M_{\mathrm{BC}}\begin{bmatrix}S_n^m(k_z)\\S_n^n(k_z)\\C_n^m(k_z)\\C_n^n(k_z)\end{bmatrix}=\begin{bmatrix}\vec{F}_n^v\cdot\hat{z}\\\vec{F}_n^v\cdot\hat{\phi}\\0\\jk\vec{F}_n^h\cdot\hat{\phi}\end{bmatrix} \tag{19}$$

while if a horizontally polarized incident wave is considered, the system to solve will be

$$M_{\mathrm{BC}}\begin{bmatrix}S_n^m(k_z)\\S_n^n(k_z)\\C_n^m(k_z)\\C_n^n(k_z)\end{bmatrix}=\begin{bmatrix}0\\\vec{F}_n^h\cdot\hat{\phi}\\-jk\vec{F}_n^v\cdot\hat{z}\\-jk\vec{F}_n^v\cdot\hat{\phi}\end{bmatrix}. \tag{20}$$

Once the coefficients $S_n^m(k_z)$ and $S_n^n(k_z)$ have been obtained, the approximated scattered field at any $\rho>a$ can be calculated from (7).

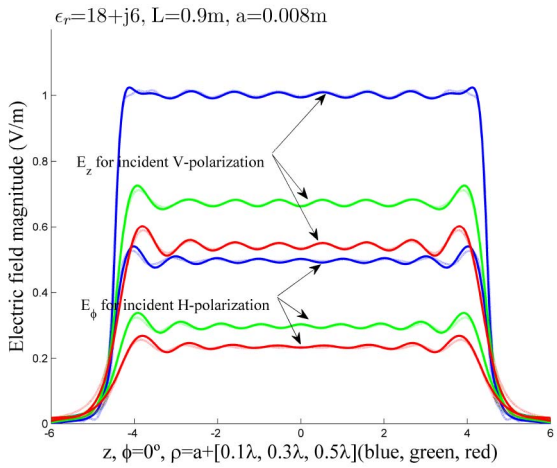

Fig. 2. Scattered electric field magnitude in the near field for cylinder 1. (Dark lines) MM method. (Light lines) Proposed approximation of this letter.

In the far-field region, as $kr\to\infty$, the solution found for the scattered field can be simplified. Considering the approximation of the outgoing cylindrical wave functions in the far-field region [3], the integral in (7) can be evaluated using the stationary phase method, and it is finally found that the scattered field in the far-field region is given by

$$\vec{E}_s\underset{kr\to\infty}{=}\sum_{n=-\infty}^{\infty}\left(S_n^m(k\cos\theta_s)\hat{\phi}+S_n^n(k\cos\theta_s)\hat{\theta}\right)\cdot e^{-j\left(\frac{n\pi}{2}\right)}e^{jn\phi_s}k\sin\theta_s\frac{e^{jkr}}{r}. \tag{22}$$

IV. Results and Discussion

Results of the proposed method, in both near- and far-field regions, have been obtained for different cylinders that approximate vegetation stalks, branches, and trunks. In general, these vegetation elements are significantly longer than thicker, with trunks and primary branches much thicker than stalks or secondary branches. Three different cylinders, i.e., 1, 2, and 3, with respective lengths of 0.9, 0.16, and 0.14 m and radii of 0.008, 0.002, and 0.026 m, representative of vegetation elements, have been considered.

The dielectric constant has significant variations depending on the growth stage of the plant and humidity [11]. A complex dielectric constant, typical of vegetation, of $18+j6$ [4] has been considered. Similar results were obtained for other values of permittivity and conductivity within the actual range for vegetation. As for the incident wave, a plane wave of 1.5, 3, or 5.3 GHz has been assumed, and vertical and horizontal polarizations have been considered.

$$M_{\mathrm{BC}}=\begin{bmatrix}0&-\frac{k_\rho^2}{k}H_n(k_\rho a)&0&\frac{k_{c\rho}^2}{k_t}J_n(k_{c\rho}a)\\k_\rho H_n'(k_\rho a)&\frac{nk_z}{ka}H_n(k_\rho a)&-k_{c\rho}J_n'(k_{c\rho}a)&-\frac{nk_z}{k_ca}J_n(k_{c\rho}a)\\-k_\rho^2H_n(k_\rho a)&0&k_{c\rho}^2J_n(k_{c\rho}a)&0\\\frac{nk_z}{a}H_n(k_\rho a)&kk_\rho H_n'(k_\rho a)&-\frac{nk_z}{a}J_n(k_{c\rho}a)&-k_{c\rho}k_cJ_n'(k_{c\rho}a)\end{bmatrix} \tag{21}$$

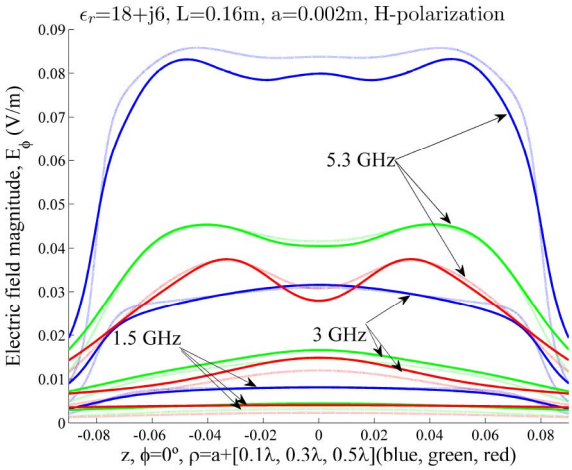

Fig. 3. Scattered electric field magnitude in the near field for cylinder 2. (Dark lines) MM method. (Light lines) Proposed approximation of this letter.

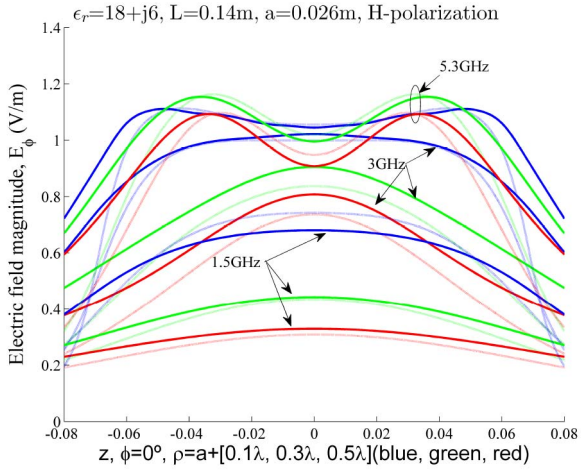

Fig. 5. Scattered electric field magnitude in the near field for cylinder 3. (Dark lines) MM method. (Light lines) Proposed approximation of this letter.

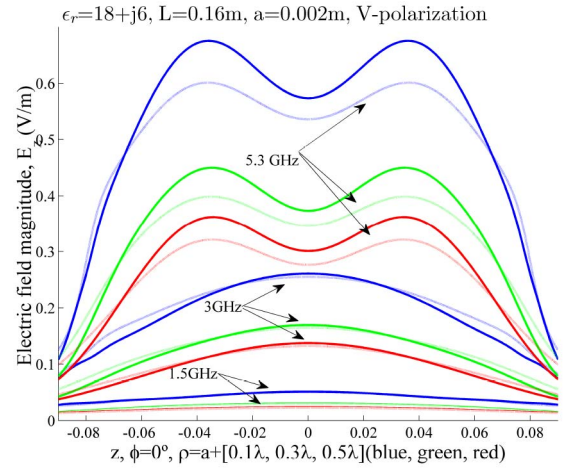

Fig. 4. Scattered electric field magnitude in the near field for cylinder 2. (Dark lines) MM method. (Light lines) Proposed approximation of this letter.

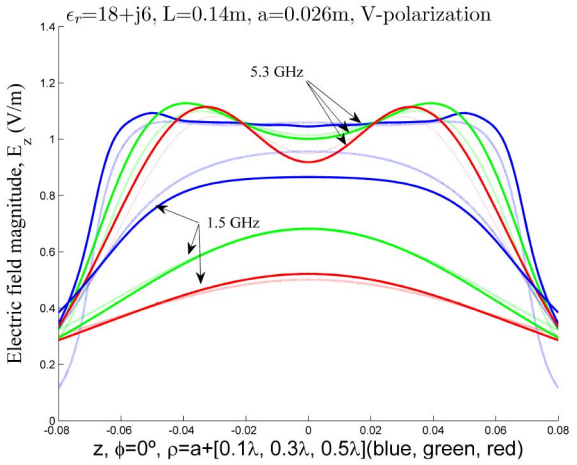

Fig. 6. Scattered electric field magnitude in the near field for cylinder 3. (Dark lines) MM method. (Light lines) Proposed approximation of this letter.

In the near-field region, the electric field has been calculated with the method proposed in this letter and using the moment method (MM). The scattered electric field in the near-field region has been calculated along constant x-lines in the ZX plane. The results are shown in Figs. 2–6.

The results of the proposed approach for cylinder 1 (Fig. 2) present very good agreement with the MM results. Although results are presented only for 3 GHz, the same accuracy was found at 1.5 and 5.3 GHz.

Figs. 3 and 4 show the results for cylinder 2 at 1.5, 3, and 5.3 GHz. Although agreement is quite good, some differences are observed between the MM results and the results of the proposed approach of this letter. These differences are due to numerical problems that occur for very small cylinder-radius-to-wavelength ratios since the matrix in (21), shown at the bottom of the next page becomes ill posed. These numerical problems may limit the applicability of the method for very thin cylinders. More studies are required to establish more definite limits.

With regard to Figs. 5 and 6, the differences observed at z-values near the edge of the cylinder are due to the scattering/radiation from the cylinder top ends and the diffraction at the borders. The approach in here does not include these contributions while the MM does. These contributions become noticeable if cylinder top ends and lateral surfaces are comparable in size, as it is the case for cylinder 3. Then, as already pointed out, the proposed approach should be used only when scattering from the cylinder top ends can or should be neglected, which is the case for most vegetation samples due to the plant structure.

Results in the far-field region are shown in Figs. 7 and 8. Bistatic scattering has been calculated for cylinders 1 and 2 with the method presented here (22) and with the infinite cylinder approximation methods as derived in [2] and [3]. Very good agreement is found, in all cases, for the specular scattering lobe, which is the most significant when analyzing scattering from vegetation.

Finally, it is important to point out the main differences between the approximation proposed in here and the previous methods used for the calculation of the scattered field by a homogeneous circular cylinder. Different methods have been employed depending on the cylinder characteristics and the point where fields are required. If the scattered field in the far field is of interest, the semianalytical infinite cylinder

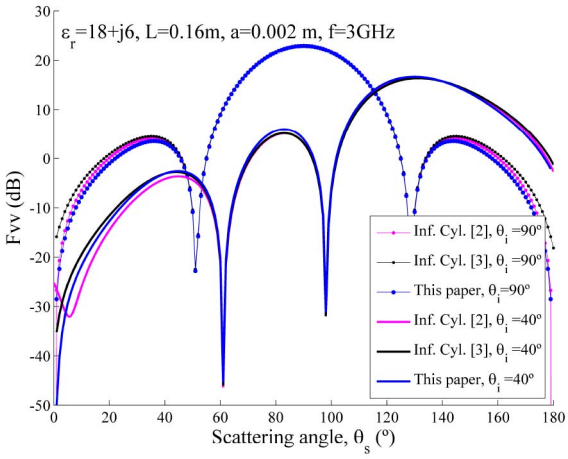

Fig. 7. VV bistatic scattered coefficient.

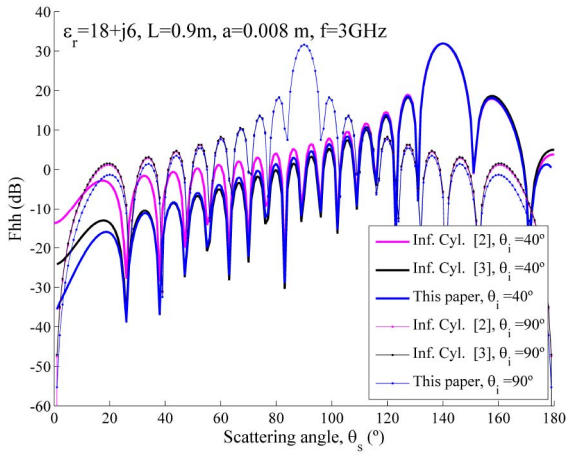

Fig. 8. HH bistatic scattered coefficient.

approximations as presented in [2] and [3] have been widely used. These approximations require a large length/radius ratio. Computationally, they are very similar to the semianalytical approach presented here, which, however, does not require a large length/radius ratio, although it neglects the scattering from the cylinder top ends. In the case that calculation of the scattered field in the near-field region was of interest, numerical methods (MM, finite-element method, etc.) would be used. These methods have proven to provide accurate results, although at the expense of large computation times. The semi-analytical approach presented allows much faster calculations with comparable accuracy if cylinder top-end scattering can be neglected. Moreover, it may be of help to account for multiple scattering between elements in the near field of each other, if discrete coherent scattering models are to be used.

V. Conclusion

A new semianalytical approximation for calculating the scattered fields from finite and homogeneous circular cylinders, in the near- and far-field regions, has been proposed. This approximation neglects the scattering/radiation from the cylinder top ends and the diffraction at the cylinder edges. Despite this, its application to plant scattering calculation is justified because of the plant structure. Scattering results, in the microwave bands, shown for cylinders with typical vegetation parameters are in good agreement with the MM results obtained for the near field and the infinite cylinder method results obtained for the far field.

References

[1] J. R. Wait, "Scattering of a plane wave from a circular dielectric cylinder at oblique incidence," *Can. J. Phys.*, vol. 33, no. 5, pp. 189–195, May 1955.

[2] M. A. Karam, Y. M. M. Antar, and A. K. Fung, "Electromagnetic wave scattering from some vegetation samples," *IEEE Trans. Geosci. Remote Sens.*, vol. 26, no. 6, pp. 799–808, Nov. 1988.

[3] L. Tsang, J. A. Kong, and K.-H. Ding, *Scattering of Electromagnetic Waves: Theories and Applications*. New York, NY, USA: Wiley, 2000.

[4] P. Matthaeis and R. H. Lang, "Microwave scattering for cylindrical vegetation components," *Progress Electromagn. Res.*, vol. 55, pp. 307–333, 2005.

[5] M. A. Karam, A. K. Fung, R. H. Lang, and N. S. Chauhan, "A microwave scattering model for layered vegetation," *IEEE Trans. Geosci. Remote Sens.*, vol. 30, no. 4, pp. 767–784, Jul. 1992.

[6] N. S. Chauhan, D. M. L. Vine, and R. H. Lang, "Discrete scatter model for microwave radar and radiometer response to corn: Comparison of theory and data," *IEEE Trans. Geosci. Remote Sens.*, vol. 32, no. 2, pp. 416–426, Mar. 1994.

[7] Y.-C. Lin and K. Sarabandi, "A Monte Carlo coherent scattering model for forest canopies using fractal-generated trees," *IEEE Trans. Geosci. Remote Sens.*, vol. 37, no. 1, pp. 440–451, Jan. 1999.

[8] S. H. Yueh, J. A. Kong, J. K. Jao, R. T. Shin, and T. L. Toan, "Branching model for vegetation," *IEEE Trans. Geosci. Remote Sens.*, vol. 30, no. 2, pp. 390–402, Mar. 1992.

[9] Q. Zhao and R. H. Lang, "Fresnel double scattering from tree branches," *IEEE Trans. Geosci. Remote Sens.*, vol. 50, no. 10, pp. 3640–3647, Oct. 2012.

[10] K. Sarabandi, F. Polatin, and F. T. Ulaby, "Monte Carlo simulation of scattering from a layer of vertical cylinders," *IEEE Trans. Antennas Propag.*, vol. 41, no. 4, pp. 465–475, Apr. 1993.

[11] F. T. Ulaby and M. A. El-Rayes, "Microwave dielectric spectrum of vegetation Part II: Dual dispersion model," *IEEE Trans. Geosci. Remote Sens.*, vol. 25, pp. 550–557, 1987.